

## Temperature dependence of fractal formation in ion-implanted *a*-Ge/Au bilayer thin films

Hou Jian-guo and Wu Zi-qin

*Fundamental Physics Center, University of Science and Technology of China, Hefei, Anhui, People's Republic of China*

(Received 6 October 1988)

Fractal regions appearing in ion-implanted (amorphous Ge)/(polycrystalline Au) bilayer thin films after annealing have been investigated. The fractal dimensions and fractal density (number of fractals per unit area) are temperature dependent. At lower temperature both the morphologies and fractal dimensions closely resemble those arising in two-dimensional diffusion-limited-aggregation (DLA) simulations. But our transmission electron micrographs show that after annealing at 100°C there are many Ge crystallites located randomly in the amorphous Ge matrix, which means that the growth mechanism is very different from that of traditional DLA's, so that a random successive nucleation model has been proposed to explain the results.

### INTRODUCTION

Recently there has been an upsurge of interest in pattern formation of nonequilibrium systems.<sup>1</sup> Of particular importance is the diffusion-limited aggregation (DLA) model proposed by Witten and Sander,<sup>2</sup> which leads to scale-invariant structures with a fractal dimension. Since then, besides a variety of fractal patterns produced by computer simulations, more and more work has been done on the observation of fractal patterns in various branches of science.<sup>3</sup> Up to now, several papers have been published about pattern formation in thin solid films,<sup>4-8</sup> and three of them deal with the growth processes during crystallization. These patterns are quite different, so different growth models have been proposed to describe the pattern formation in alloy films during crystallization;<sup>6-8</sup> for example, a model which is different from DLA was presented by Deutscher and Lareah<sup>8</sup> to deal with a kind of nonfractal pattern (dense branch morphology) in eutectic Al-Ge alloy films. These models neither correlate the patterns with the microstructure in detail nor systematically consider the temperature dependence of pattern formation. Obviously, these two factors are important for an understanding of the actual growth mechanism. In this paper, we report the investigation of the fractal regions appearing in Si-ion-implanted [amorphous Ge (*a*-Ge)]/[polycrystalline Au (*p*-Au)] bilayer films after annealing and focus our attention on the microstructure in the fractal region and the effects of the annealing temperature. A possible mechanism which can be called random successive nucleation (RSN) is discussed, based on structural and compositional analyses.

### EXPERIMENT

Specimens were prepared by evaporation on flash-cleaved NaCl(100) crystals in vacuum with a pressure of  $3 \times 10^{-5}$  Torr at room temperature. We deposited Au first and then Ge without breaking the vacuum. The thicknesses of *a*-Ge and *p*-Au films are about 25 and 30 nm, respectively. As-evaporated films were then implant-

ed with Si ions at room temperature with a dose of  $5 \times 10^{14}$  Si/cm<sup>2</sup>. To induce the intermixing of Au and Ge effectively, the incident energy of Si ions was chosen as 40 keV, so that the projected peak range should be approximately equal to the thickness of the top Ge layer. The beam-current density during implantation was less than 1  $\mu$ A/cm<sup>2</sup> to avoid significant target heating. During implantation, the penetration of energetic Si ions passing through the interface of Au/Ge caused Au atoms to move outward and Ge atoms inward. In addition, a thin layer of mixed Au-Ge was formed by collision mixing and recoil mixing.<sup>9</sup> After implantation, all specimens were annealed in vacuum at different temperatures. After floating the bilayers in distilled water and putting them on grids, they were examined by an H-800 and a JEOL-4000 transmission electron microscope (TEM) operating at 200 and 400 kV, respectively. Quantitative analyses were done by use of an EDAX-9100 energy-dispersive system (EDS).

### RESULTS

Before annealing, TEM observation shows that the film is homogeneous in morphology and consists of amorphous Ge and polycrystalline Au. After annealing at 100°C for 4 h, large bright DLA-like regions are distributed throughout the film (Fig. 1). There are some interesting features shown in this TEM image, in which some regions, for example *A* and *B*, grow away from each other, whereas in some other regions, for example *C* and *D*, they grow together, resembling a single DLA cluster.

The selected-area diffraction (SAD) patterns of these bright regions indicate that the Ge has been crystallized, whereas in the SAD patterns of the uniform dark matrix, there are no Ge diffraction rings. Local energy-dispersive x-ray analysis shows that the dark regions are Au-rich regions and the bright regions are Ge-rich regions. The concentrations of Au and Ge in different regions are listed in Table I. The data were obtained by averaging over four analysis points. Quantitative analysis and selected-area diffraction patterns indicate the occurrence of a la-

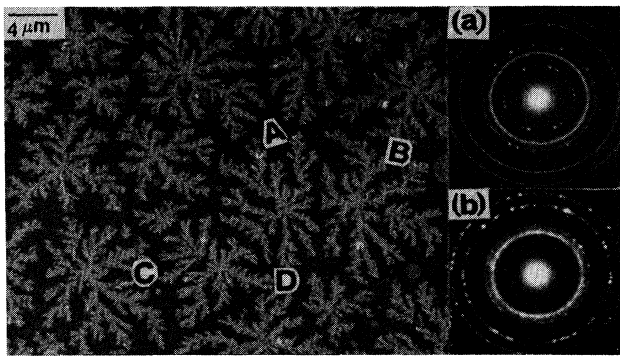


FIG. 1. TEM image and selected-area diffraction patterns after annealing at 100 °C for 4 h. Large bright DLA-like regions are formed. (a) SAD pattern of fractal region indicates that they consist of Ge crystalline grains. (b) SAD pattern of dark matrix shows no Ge diffraction rings.

teral diffusion of Ge atoms, i.e., Ge aggregates into fractal-like regions.

After annealing at 200 and 300 °C for 0.5 h, the individual bright regions are also DLA-like, but are more dense and have thicker limbs as compared with those annealed at 100 °C. When the temperature reaches 350 °C, close to the eutectic temperature of Au-Ge, irregular islandlike bright regions appear after annealing for 2 min (Fig. 2). In this figure, there are also a few round grey regions which may be considered as local melting when the temperature is above the eutectic.

The average radius of gyration of the bright regions decreases from 4.2 to 0.8  $\mu\text{m}$  when the temperature increases from 100 to 350 °C. The data were obtained by averaging over ten regions at each temperature (Table II). Figure 3 shows that the number of bright regions per unit area increases with the increasing annealing temperature.

In order to illustrate the scale-invariant nature of such bright regions, images taken of individual regions were digitized by use of a PDS-1010M microdensitometer at  $256 \times 256$  pixels. A threshold criterion was then applied to separate pixels in the bright regions from the background. Figure 4 shows the digitally reproduced images of bright regions after annealing at different temperatures. The quantitative analysis of these digitized images has been carried out by the density-density correlation function method<sup>2</sup> and the sandbox method.<sup>10</sup> The results are listed in Table II, and the data obtained by the above two methods are consistent. From Table II, we know that the fractal dimensions are temperature dependent.

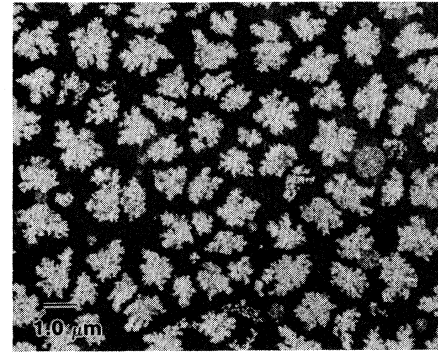


FIG. 2. TEM image of the film after annealing at 350 °C for 2 min. Many irregular islandlike bright regions are formed.

When temperature increases from 100 to 350 °C, the fractal dimension increases from 1.69 to 1.95, while the spacing range in which correlation functions  $C(r)$  conforming to a power-law relationship decreases with increasing temperature.

To understand the growth mechanism, it is necessary to know the microstructure of the fractal regions. Figure 5 is a high-resolution TEM (HREM) image taken from one of the fractal regions shown in Fig. 1, from which we can see many imperfect crystallites with sizes of several nm located randomly. It is worth noting that there are some amorphous domains (arrowed) still existing in fractal regions, in contrast to the result that new crystallites nucleate at the Al/Ge interface.<sup>8</sup> In specimens annealed at 300 °C, the microstructure of the fractal regions (Fig. 6) is very different from that shown in Fig. 5. Although some defects and microtwins can be found, the crystal grains are much larger and more perfect, and no amorphous domains can be found.

## DISCUSSION

When an *a*-Ge film contacts a Au film, the crystallization temperature of Ge decreases remarkably by heterogeneous nucleation at the Au/Ge interface, and limited mass transport takes place in some regions; therefore, a small amount of fractal-like regions can be observed.<sup>11</sup> After ion implantation, crystallization temperature decreases further and significant diffusion of Ge takes place.<sup>12</sup> As a result, large and well-ramified fractal regions are formed everywhere. This may be due to the higher instability around the interface caused by the energy deposition of incident ions.

TABLE I. Concentrations of Au and Ge in different regions before and after annealing at 100 °C. Experimental conditions: accelerating voltage, 200 kV; beam current, 10  $\mu\text{A}$ ; x-ray takeoff angle, 68°; x-ray photon-counting time, 60 s.

Element	Nonannealed film		Bright region of annealed film		Dark region of annealed film	
	Au	Ge	Au	Ge	Au	Ge
Concentration (at. %)	58.9	41.1	32.6	67.4	89.7	10.1

TABLE II. Temperature dependence of fractal dimension ( $D$ ), average radius of gyration ( $R$ ), and linear spacing range ( $r$ ) in the  $\ln C(r) - \ln r$  curve.  $D_c$ , correlation-function method;  $D_s$ , sandbox method.

$T$ ( $^{\circ}\text{C}$ )	$D_c$	$D_s$	$R$ ( $\mu\text{m}$ )	Spacing ranges ( $\mu\text{m}$ )
100	$1.69 \pm 0.01$	$1.69 \pm 0.05$	$4.2 \pm 0.4$	$0.34 \leq r \leq 1.51$
200	$1.72 \pm 0.01$	$1.71 \pm 0.01$	$2.5 \pm 0.5$	$0.28 \leq r \leq 0.97$
300	$1.77 \pm 0.01$	$1.76 \pm 0.01$	$1.5 \pm 0.3$	$0.16 \leq r \leq 0.52$
350	$1.95 \pm 0.02$	$1.93 \pm 0.03$	$0.8 \pm 0.1$	$0.03 \leq r \leq 0.13$

Obviously, the similarity of morphologies between DLA clusters and the bright fractal region observed in our ion-implanted  $a$ -Ge/Au specimen does not mean a similar growth mechanism. In the HREM image (Fig. 5), the presence of many Ge grains and amorphous domains located randomly within the fractal region indicate that random successive nucleation (RSN) of Ge plays a dominant role. The present results lead us to propose a revised growth mechanism which is similar to the model proposed recently by Duan and Wu.<sup>13</sup> At the early stage of  $a$ -Ge crystallization, some Ge nuclei or "seeds" nucleate at those favored sites located at the Au/Ge interface.<sup>12,14</sup> From TEM images, we know that these primary nuclei that determine the number of fractals are a few micrometers apart. As mentioned above, a layer of mixed Au-Ge was formed after ion implantation, and TEM analysis indicates a lateral diffusion of Ge. This leads us to make an assumption that the growth of these nuclei is limited by the diffusion of Ge through the passages between Au grain boundaries. At the same time, the latent heat released by crystallization leads to a rise in temperature in surrounding regions, and this temperature field propagates fast, since the thermal diffusion is much faster than the atomic diffusion, so that the heat flow can stimulate new nuclei appearing randomly in nearby regions for further diffusion-limited crystallites growth. Obviously, these stimulated nuclei can also produce a local temperature rise and act as new crystallization centers. During annealing, the above processes repeat many times until fractal regions are formed, so that the appearance of fractal regions in the  $a$ -Ge/Au system is mainly due to the random successive nucleation process, which constructs the skeleton of fractal regions.

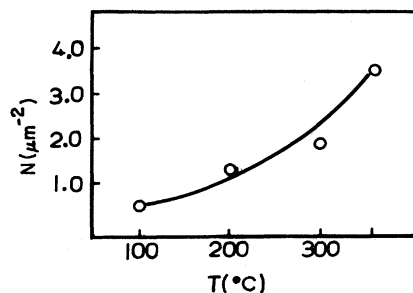


FIG. 3. Number of fractal regions per unit area ( $N$ ) vs annealing temperature ( $T$ ).

Based on the HREM observation, we can discuss the growth mechanism in some detail. From Fig. 5, we found that the largest distance between two neighboring crystallites is less than 10 nm, which means that the growth step of fractal regions is also less than 10 nm. Comparing with the average gyration radius ( $4.2 \mu\text{m}$ ), we can estimate that the number of crystallites within each fractal region is about  $10^5$ , which is large enough to form a fractal. Figure 7 shows the morphology of the film after annealing at  $100^{\circ}\text{C}$  for 0.5 h. At this early growth stage, we can see small bright fractal regions surrounded by narrow dark regions. Quantitative analysis indicates that the dark regions are Au-rich regions. This means that accompanying the nucleation and growth of Ge crystallites, the diffusion of Ge takes place and is stimulated by the local temperature rise. Because the growth step is very small, it is easy to speculate that only those tip branches which are close to the (Au-rich region)/(amorphous matrix) border can grow further and faster, and finally form well-ramified fractal regions.

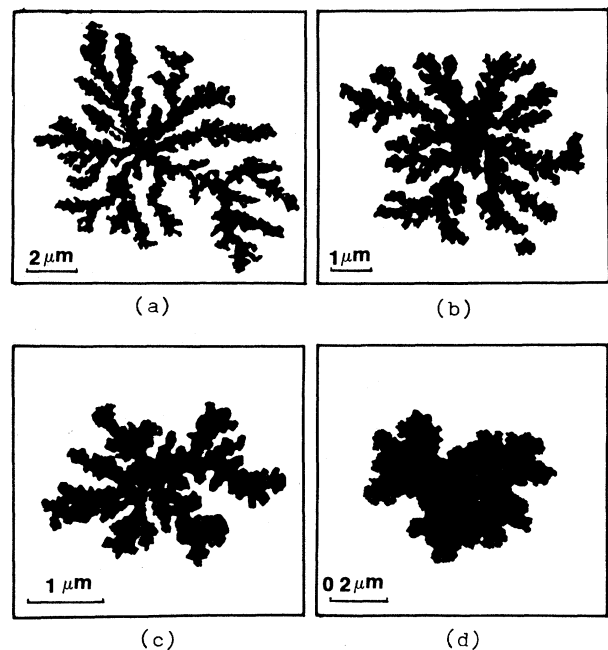


FIG. 4. Digitally reproduced TEM images of fractal regions at different annealing temperatures. (a)  $100^{\circ}\text{C}$ , 4 h; (b)  $200^{\circ}\text{C}$ , 0.5 h; (c)  $300^{\circ}\text{C}$ , 0.5 h; (d)  $350^{\circ}\text{C}$ , 2 min.

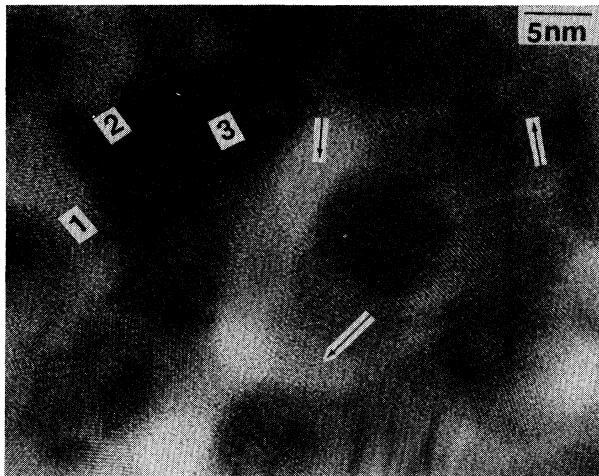


FIG. 5. HREM image from a part of the fractal region shown in Fig. 1. Many crystallites located randomly. We can find many twins and defects within these crystallites. 1, 2, and 3 are multiple twins—they are connected at nearly the same angle ( $70.5^\circ$ ). Arrows indicate that some amorphous domains still exist in fractal regions.

From the above discussion, we can conclude that DLA-like fractal structure can be formed by spreading from center in real systems even when the diffusion length is relatively short, in contrast to the traditional DLA model in which particles diffuse inward from an infinite distance.

In the computer simulations, limb thickening can be achieved by lowering the sticking probabilities or allowing the particles to relax to occupy those sites with more neighbors,<sup>4,15,16</sup> and the latter reflects the effect of surface tension in real systems. In our experimental system,

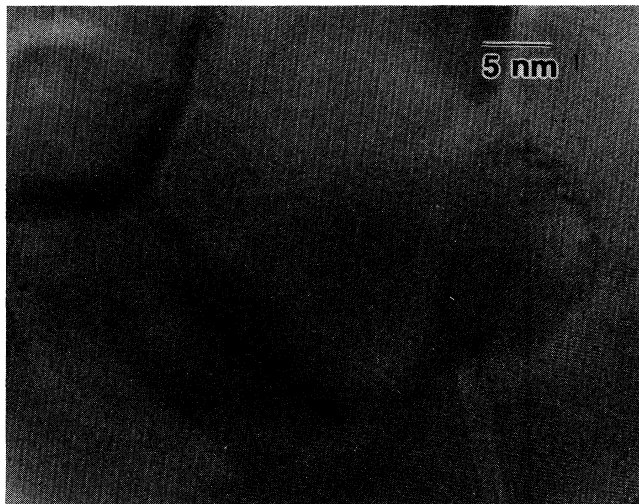


FIG. 6. HREM image from a part of the fractal region after annealing at  $300^\circ\text{C}$  for 0.5 h. The crystallites are much larger and more perfect.

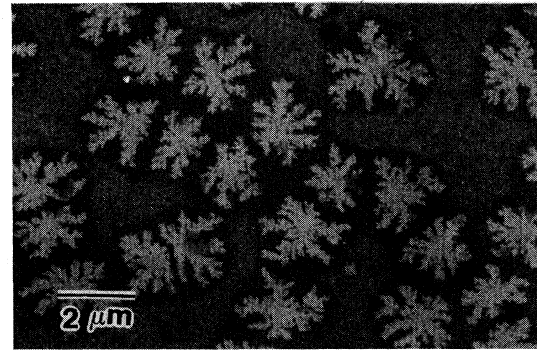


FIG. 7. At the early growth stage of annealing at  $100^\circ\text{C}$  for 0.5 h, the small bright fractal regions are surrounded by narrow Au-rich regions.

the effects caused by the surface tension are expected to be small because the Au and Ge are polycrystalline with randomly distributed orientations.

The appearance of thicker fractal regions can be also explained by our growth mechanism. At lower temperature, the diffusion-limited crystallites growth rate is low, so that some Ge crystallites cannot grow large enough to contact each other, and amorphous domains remain between them, as shown in Fig. 5. At higher temperature, the higher crystal-growth rate leads to the larger grains in fractals; moreover, the crystallites can also coalesce to form larger grains. But the main factor in this case is that more stimulated nuclei appear randomly around the previous crystallization centers with the increasing temperature. As a result of the above two factors, the fractal regions became thicker and have fewer limbs.

Fractal dimensions must reflect the correlations existing in the formation of fractals. We believe that in the *a*-Ge/Au system the correlation is determined by the random successive nucleation process; as discussed above, such a process is temperature dependent, so that the fractal dimensions of the bright regions increase with increasing temperature.

In summary, we can describe the basic features leading to the appearance of fractals in annealed *a*-Ge/Au bilayer films as follows: (1) heterogeneous nucleation of primary Ge nuclei in favored sites at the Au/Ge interface, (2) local temperature rise around these sites, (3) random successive nucleation in the nearby regions of previous sites, (4) diffusion-limited crystallite growth, and (5) the higher instability required for perfect fractal growth is presented by the ion implantation.

#### ACKNOWLEDGMENTS

We greatly appreciate partial support from the Third World Academy of Sciences. We thank also Dr. Chen Jun of the Microstructure Physics Laboratory, Nanjing University, for the HREM examination, and S. Y. Zhang and Q. Pan of the Structure Research Laboratory, University of Science and Technology of China (USTC), for their kind help.

- <sup>1</sup>L. P. Kadanoff, *Phys. Today* **39** (2), 6 (1986).
- <sup>2</sup>T. A. Witten and L. M. Sander, *Phys. Rev. Lett.* **47**, 1400 (1980); *Phys. Rev. B* **27**, 5686 (1983).
- <sup>3</sup>L. M. Sander, *Nature* **322**, 789 (1986).
- <sup>4</sup>W. T. Elam, S. A. Wolf, J. Sprague, D. U. Gubser, D. van Vechten, G. L. Barz, Jr., and Paul Meakin, *Phys. Rev. Lett.* **54**, 701 (1985).
- <sup>5</sup>B. X. Liu, L. J. Huang, K. Tao, C. H. Shang, and H. D. Li, *Phys. Rev. Lett.* **59**, 75 (1987).
- <sup>6</sup>Duan Jian-zhang and Wu Zi-qin, *Solid State Commun.* **64**, 1 (1987).
- <sup>7</sup>Gy. Radnoczi, T. Vicsek, L. M. Sander, and D. Grier, *Phys. Rev. A* **35**, 4012 (1987).
- <sup>8</sup>G. Deutscher and Y. Lareah, *Phys. Rev. Lett.* **60**, 1510 (1988).
- <sup>9</sup>B. M. Paine, *Nucl. Instrum. Methods, Phys. Res. B* **7/8**, 661 (1985).
- <sup>10</sup>R. Forrest, *J. Phys. A* **12**, L109 (1979).
- <sup>11</sup>Hou Jian-guo and Wu Zi-qin, *Acta Phys. Sinica* **37**, 1735 (1988).
- <sup>12</sup>Hou Jian-guo and Wu Zi-qin, *Thin Solid Films* **172** (1989).
- <sup>13</sup>Duan Jian-zhang, Li Yan, and Wu Zi-qin, *Solid State Commun.* **65**, 7 (1988).
- <sup>14</sup>Zhang Ren-ji and Wu Zi-qin, *Acta Phys. Sinica* **35**, 365 (1986).
- <sup>15</sup>P. Meakin, *Phys. Rev. A* **27**, 1495 (1983).
- <sup>16</sup>T. Vicsek, *Phys. Rev. Lett.* **53**, 2281 (1984).

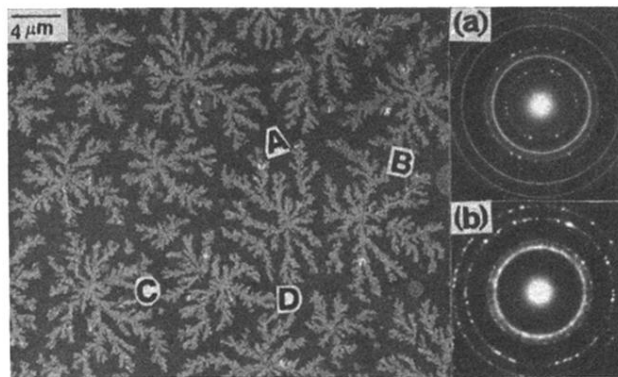


FIG. 1. TEM image and selected-area diffraction patterns after annealing at 100°C for 4 h. Large bright DLA-like regions are formed. (a) SAD pattern of fractal region indicates that they consist of Ge crystalline grains. (b) SAD pattern of dark matrix shows no Ge diffraction rings.

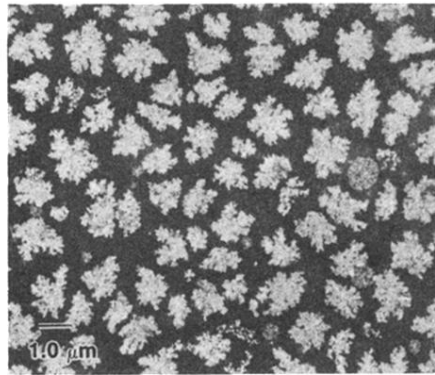


FIG. 2. TEM image of the film after annealing at 350°C for 2 min. Many irregular islandlike bright regions are formed.

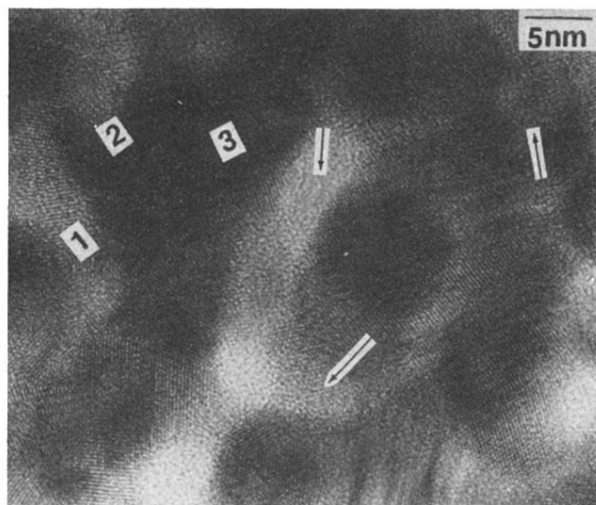


FIG. 5. HREM image from a part of the fractal region shown in Fig. 1. Many crystallites located randomly. We can find many twins and defects within these crystallites. 1, 2, and 3 are multiple twins—they are connected at nearly the same angle ( $70.5^\circ$ ). Arrows indicate that some amorphous domains still exist in fractal regions.



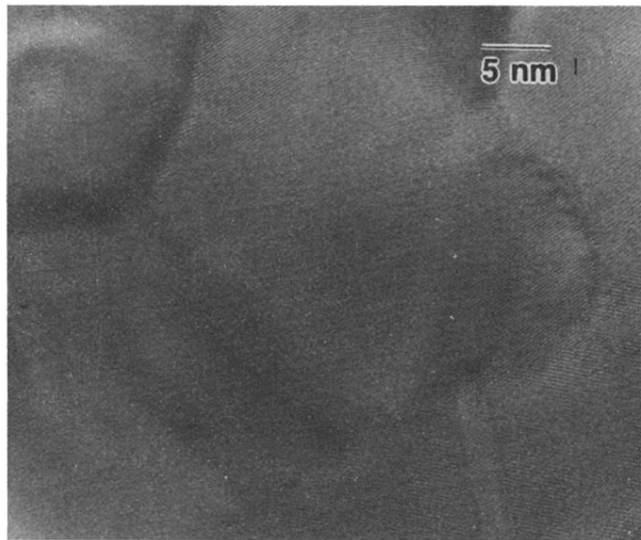


FIG. 6. HREM image from a part of the fractal region after annealing at 300°C for 0.5 h. The crystallites are much larger and more perfect.

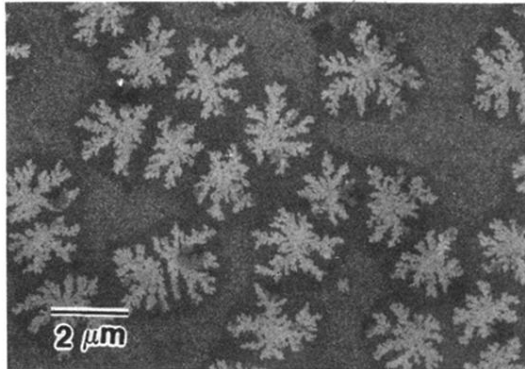


FIG. 7. At the early growth stage of annealing at 100°C for 0.5 h, the small bright fractal regions are surrounded by narrow Au-rich regions.